New ruthenium–tin clusters with bulky ligands. Crystal and molecular structures of $[Ru_2(CO)_6(\mu\text{-}SnR_2)(\mu\text{-}Ph_2PCH_2PPh_2)]$, $[Ru_3(CO)_9(\mu\text{-}SnR'_2)_3]$, $[Ru_3(CO)_9(\mu\text{-}SnR_2)(\mu\text{-}SnR'_2)_2]$ and $[Ru_3(CO)_9(\mu\text{-}SnR_2)_2(\mu\text{-}SnR'_2)]$ [R = $CH(SiMe_3)_2$, R′ = $C_6H_2Pr^i_3$-2,4,6] *

Christine J. Cardin,[a] David J. Cardin,[a] Maire A. Convery,[b] Zbigniew Dauter,[c] Dieter Fenske,[d] Michael M. Devereux[b] and Michael B. Power[b]

[a] *Department of Chemistry, University of Reading, Whiteknights, Reading, Berkshire RG6 6AD, UK*
[b] *Department of Chemistry, Trinity College, University of Dublin, Dublin 2, Ireland*
[c] *European Molecular Biology Laboratory, c/o DESY, Notkestrasse 85, D-2000 Hamburg 52, Germany*
[d] *Institut für Anorganische Chemie der Universität, Engesserstrasse, Geb. Nr. 30.45, D-76128 Karlsruhe, Germany*

The first heterometallic clusters containing the SnR'_2 (R′ = 2,4,6-triisopropylphenyl) moiety have been prepared. Triruthenium dodecacarbonyl reacted at low temperatures with SnR'_2 or, at higher temperatures, with its trimer $(SnR'_2)_3$ to give both $[Ru_3(CO)_{10}(\mu\text{-}SnR'_2)_2]$ **1** and $[Ru_3(CO)_9(\mu\text{-}SnR'_2)_3]$ **2**. Reaction of the pentametallic species $[Ru_3(CO)_{10}(\mu\text{-}SnL_2)_2]$ [L = R = $CH(SiMe_3)_2$ **3** or R′] with SnR'_2 or SnR_2 respectively afforded the hexametallic clusters $[Ru_3(CO)_9(\mu\text{-}SnR_2)(\mu\text{-}SnR'_2)_2]$ **4** and $[Ru_3(CO)_9(\mu\text{-}SnR_2)_2(\mu\text{-}SnR'_2)]$ **5**. In the reaction of $[Ru_3(CO)_{12}]$ with SnR_2 the hexametallic cluster $[Ru_3(CO)_9(\mu\text{-}SnR_2)_3]$ **6** has now been isolated in addition to the previously reported Ru_3Sn_2 cluster. The trimer $(SnR'_2)_3$ also reacted with $[Ru_3(CO)_{10}(dppm)]$ (dppm = $Ph_2PCH_2PPh_2$) to give $[Ru_3(CO)_8(\mu\text{-}SnR'_2)_2(dppm)]$ **7**, whereas with SnR_2 the product was $[Ru_2(CO)_6(\mu\text{-}SnR_2)(\mu\text{-}dppm)]$ **8**. Compound **7** can also be obtained by the reaction of **2** with dppm, using sodium–benzophenone to activate the cluster. Reaction of the dodecacarbonyl with $Sn[CH(PPh_2)_2]_2$ or its lead analogue surprisingly did not yield a mixed cluster, but afforded a rapid and quantitative route to $[Ru_3(CO)_{10}(dppm)]$. Compound **2** behaves similarly, yielding **7** again in high yield. The crystal and molecular structures of **2**, **4**, **5** and **8** have been determined. In compounds **2**, **4** and **5**, the ruthenium triangle and the three tin atoms form a planar array. A detailed comparison of ligand steric effects is made. In **8** the metal atoms and the two P atoms are coplanar, with a long Ru–Ru vector bridged by the R_2Sn group and the diphosphine [2.954(2) Å]. The structure of **4** is unusual, the characteristic aryltin twist on only two of the three tin atoms generating chirality, resulting in a spiral packing in space group $P6_5$. This structure was determined both diffractometrically and using two different image-plate systems, and the results are remarkably consistent in all three cases.

Clusters of the transition metals with main-group elements have aroused much recent interest, and are the subject of a substantial review.[2] Tin–transition metal compounds form a substantial part of these studies,[3] but other main-group elements are well represented.[4] We have reported on the use of the low-valent tin reagent SnR_2 [R = $CH(SiMe_3)_2$] in the synthesis of heterometallic clusters of iron,[5] ruthenium,[6] osmium[7] and iridium.[8] We now show that related diorganotin(II) species $(SnR'_2)_n$ (R′ = $C_6H_2Pr^i_3$-2,4,6; n = 1 or 3) can also be used in the preparation of heterometallic ruthenium clusters with nuclearities of five or six. These are the first heterometallic clusters incorporating the SnR'_2 group. There are, however, clear differences between these diorganotin(II) reagents (with R or R′) and $Sn[CH(PPh_2)_2]_2$ which affords no stable tin–ruthenium cluster, but gives rapid and quantitative transfer of the diphosphine group to the transition-metal cluster.

Discussion

For analytical and spectroscopic data on the new compounds see Tables 1 and 2.

In a recent paper we described the different behaviour of bis[bis(trimethylsilyl)methyl]tin with the dodecacarbonyls of the Group 8 triad.[6] Whereas the osmium compound does not react unless activated and the iron species undergoes partial cluster breakdown, the ruthenium carbonyl affords pentametallic clusters rapidly and in high yield. The related bis(aryl)tin species[9,10] SnR'_2 (R′ = 2,4,6-triisopropylphenyl) reacts similarly with the ruthenium species, equation (1). The reaction can

$$[Ru_3(CO)_{12}] + SnR'_2 \longrightarrow \underset{\mathbf{1}}{[Ru_3(CO)_{10}(\mu\text{-}SnR'_2)_2]} + \underset{\mathbf{2}}{[Ru_3(CO)_9(\mu\text{-}SnR'_2)_3]} \quad (1)$$

be brought about either by treatment of the carbonyl with the trimeric tin species in tetrahydrofuran (thf) under gentle reflux, or using the dissociated tin compound (probably essentially a dimer) in thf or in diethyl ether at −50 °C. In the case of the dissociated species it is not possible to be precise about stoichiometric ratios because of the slow trimerisation in solution (see Experimental section). In both these cases a small quantity of a third, purple cluster was obtained, but this has not been characterised. It is probable, although it has not been definitely established, that both of these reactions proceed *via* the dissociated tin species which forms deep red solutions. On warming, the orange trimeric species affords deep red solutions,

* Metal cluster expansion by addition of low valent Group 14 reagents. Part 5.[1]

Table 1 Analytical data for new compounds

Compound	Colour	M.p. (°C)	Analyses[a] C	H	R_f (TLC)
1 $[Ru_3(CO)_{10}(\mu\text{-}SnR'_2)_2]$	Orange	135.4 (decomp.)	52.30 (51.45)	6.15 (5.65)	0.36[b]
2 $[Ru_3(CO)_9(\mu\text{-}SnR'_2)_3]$	Red	134.6 (decomp.)	56.60 (55.80)	7.00 (6.55)	0.42[b]
4 $[Ru_3(CO)_9(\mu\text{-}SnR_2)(\mu\text{-}SnR'_2)_2]$	Red	168	49.45 (48.80)	6.60 (6.40)	0.8[c]
5 $[Ru_3(CO)_9(\mu\text{-}SnR_2)_2(\mu\text{-}SnR'_2)]$	Red	215.2 (decomp.)	41.05 (41.15)	6.30 (6.30)	0.75[c]
6 $[Ru_3(CO)_9(\mu\text{-}SnR_2)_3]$	Yellow	150.6 (decomp.)	33.75 (32.80)	6.90 (6.15)	0.8[c]
7 $[Ru_3(CO)_8(\mu\text{-}SnR'_2)_2(dppm)]$[d]	Orange	160.65 (decomp.)	56.85 (56.90)	5.85 (5.80)	
8 $[Ru_2(CO)_6(\mu\text{-}SnR_2)(dppm)]$[e]	Pale yellow	180.85 (decomp.)	45.35 (47.80)	5.75 (5.85)	

[a] Calculated figures in parentheses. [b] Silica (hexane–dichloromethane, 95:5). [c] Silica (hexane). [d] P 3.15 (3.15)%. [e] P 5.2 (5.0)%.

Table 2 Spectroscopic data for the new complexes

Compound	IR $\tilde{\nu}$(CO)/cm^{-1}	^{1}H NMR (δ, J/Hz)[a]
1	[b] 2092m, 2045m, 2035m, 2015s, 2000m, 1992m	[c] 1.01 (m), 1.18 (d, J = 7.08), 2.79 (t, J = 7.08), 3.23 (m, J unresolved), 6.96 (s)
	[d] 2090m, 2050s, 2035s, 2015s, 1995s, 1985 (sh), 1845 (br)	[e] 1.09 (d, 6 H, J = 6.83), 1.12 (m, 12 H), 2.66 (st, 1 H, J = 6.83), 3.51 (m, 2 H), 7.06 (s, 2 H)
2	[b] 2030s, 2000s, 1990s	[c] 1.13 (m, 12 H), 1.19 (d, 6 H, J = 6.59), 2.79 (spt, 1 H, J = 6.59), 3.36 (spt, 2 H), 6.96 (s, 2 H)
	[d] 2020m, 1997s, 1990m	
4	[b] 2030s, 2000s, 1990s	[c] 0.215 (s, 18 H), 0.23 (s, 18 H), 0.7 (m, 48 H), 1.1 (d, 24 H, J = 8.75), 2.72 (spt, 4 H, J = 8.75), 3.19 (spt, br, 8 H), 6.87 (m, 8 H)
	[d] 2025s, 2000s, 1990s	[e] 0.32 (d, 36 H), 0.78 (m, 48 H), 1.18 (d, 24 H, J = 7.08), 2.79 (spt, 4 H, J = 7.08), 3.43 (spt, br, 8 H), 6.96 (s, 8 H)
5	[b] 2025s, 2000s, 1990s	[c] 0.215 (m, 72 H), 0.92 (m, br, 24 H), 1.1 (d, 12 H, J = 7.5), 2.70 (spt, 2 H, J = 7.5), 2.85 (spt), 3.0 (spt), 3.21 (spt), 6.88 (m, 4 H)
	[d] 2025s, 2000s, 1990s	
6	[b] 2060m, 2040m, 1998s	[e] 0.235 (s), 0.287 (s), 0.32 (s)
	[d] 2060m, 2038m, 1995s	
7	[b] 2058m, 2030m, 1986s, 1973s, 1955m, 1913w	[c] 1.15 (m), 1.21 (d, 24 H, J = 7.38), 2.78 (spt, 4 H, J = 7.38), 3.71 (spt, br, 8 H), 4.23 (t, 2 H, J = 9.8), 6.74 (m, br, 20 H), 7.29 (m, 8 H)
	[d] 2055w, 2050m, 2016s, 1998s, 1985 (sh), 1970m, 1929w	
8	[b] 2045w, 2009s, 1995s, 1955s	
	[d] 2010s, 1980s, 1967m	

[a] Shifts downfield from internal $SiMe_4$. [b] KBr disc. [c] In $CDCl_3$, 250 MHz. [d] In CH_2Cl_2 solution. [e] In C_6D_6 80 MHz.

and TLC analysis shows no product formation prior to this stage. The bis(tin) cluster shows a single, sharp bridging carbonyl stretch in the IR spectrum which is otherwise very similar to the spectrum of $[Ru_3(CO)_{10}(\mu\text{-}SnR_2)_2]$ **3** [R = $CH(SiMe_3)_2$]. The structure of the latter was confirmed by a single-crystal analysis,[5a] as was that of the osmium analogue $[Os_3(CO)_{10}(\mu\text{-}SnR_2)_2]$ [R = $CH(SiMe_3)_2$], and the three are clearly isostructural.

The second product in equation (1) has the composition of three tin atoms (and associated ligands) bridging the three sides of a ruthenium triangle, an analogous product not having been detected earlier for the case of the SnR_2 reagent. The IR spectrum of **2** in contrast to **1** has three sharp terminal absorptions, but no bridging carbonyl frequencies (both in the solid and in solution), suggesting an $Ru_3(\mu\text{-}SnR'_2)_3$ arrangement. Molecules having a similar structure, with three sides of a metal carbonyl triangle bridged by main-group elements, have previously been reported for Ru_3 or Os_3 triangles and $GeMe_2$ bridges,[11–13] and for Os_3 with $SiMe_2$ bridges.[14] These species were unexpectedly obtained in low yields (1–2%) in thermal reactions of Si_2Me_5H or $[M(CO)_4(GeMe_3)_2]$ and do not have the same symmetrical structure. An X-ray analysis of $[Ru_3(CO)_9(\mu\text{-}GeMe_2)_3]$[13,14] revealed an idealised D_{3h} (6*m*2) molecular symmetry, which is suggested for **2** by the carbonyl region of the IR spectrum (see above). Such asymmetry in trinuclear clusters composed of similar units has been previously observed, for example in the solid-state structure of $(SnR'_2)_3$. This is an interesting case, since although the structure is composed of twelve scalene triangles at room temperature[10] at −50 °C the crystal undergoes ordering to one of three isosceles triangles.[15]

In view of the rather lower bulk and higher nucleophilicity of R compared with R′ (see below) it seemed surprising that the hexametallic Ru_3Sn_3 cluster was not formed in the reaction of the ruthenium carbonyl with the dialkyltin.[5a] A re-examination of the reaction of SnR_2 with $[Ru_3(CO)_{12}]$ in ether–toluene showed that it proceeds analogously to equation (1). The new compound $[Ru_3(CO)_9(\mu\text{-}SnR_2)_3]$ **6** was characterised on the basis of elemental analysis, IR and NMR spectroscopy, and forms bright yellow crystals. Both the alkyltin compounds **3** and **6** are highly soluble in hydrocarbon solvents, and require careful separation by TLC; the presence of **6** can be overlooked when mixed with a greater quantity of **3**.

The isolation of compounds of both metal framework stoichiometries Ru_3Sn_2 and Ru_3Sn_3 for tin atoms bearing either alkyl or aryl substituents suggests the possibility of making clusters with both SnR_2 and SnR'_2 groups. The reactions (2) and (3) can be carried out either in toluene just below reflux temperature (2) or in the same solvent at 60 °C (3). Both products are obtained in high yield as red, stable,

$$[Ru_3(CO)_{10}(SnR_2)_2] + \tfrac{1}{3}(SnR'_2)_3 \longrightarrow [Ru_3(CO)_9(SnR_2)_2(SnR'_2)] \quad (2)$$
5

$$[Ru_3(CO)_{10}(SnR'_2)_2] + SnR_2 \longrightarrow [Ru_3(CO)_9(SnR_2)(SnR'_2)_2] \quad (3)$$
4

crystalline solids. They show three sharp carbonyl stretching bands in the IR spectra (in solution or as solids), like **2** and **6**, and are easily characterised from their NMR spectra, which show bands for both alkyl- and aryl-tin substituents with appropriate integrations. An interesting detail relating to the relative bulk of the two tin moieties is revealed by these NMR data. Thus the isopropyl substituents in **5** show hindered rotation to the extent of broadening of the septet and doublet of the *o*-isopropyl groups, whereas for **4** with two of the bulkier SnR'_2 groups there are three fully resolved septets (at 270 MHz) and the splitting of the diastereotopic methyl resonances (of the R groups) is much greater for the latter compound.

Both tin reagents also react with $[Ru_3(CO)_{10}(dppm)]$ [dppm = bis(diphenylphosphino)methane], but not in similar ways, equations (4) and (5). Reaction (4) proceeds analogously

$$[Ru_3(CO)_{10}(dppm)] + (SnR'_2)_3 \longrightarrow [Ru_3(CO)_8(\mu\text{-}SnR'_2)_2(\mu\text{-dppm})] \quad (4)$$
7

$$[Ru_3(CO)_{10}(dppm)] + SnR_2 \longrightarrow [Ru_2(CO)_6(\mu\text{-}SnR_2)(\mu\text{-dppm})] \quad (5)$$
8

to (2), and compound **7** can indeed also be obtained by reaction of **1** with dppm, but then requires activation with sodium–benzophenone, both routes affording good yields. A third route is also possible, using **1** and $Sn[CH(PPh_2)_2]_2$; for reactions of this reagent see below. The osmium analogue of **7**, but having alkyltin groups, $[Os_3(CO)_8(\mu\text{-}SnR_2)_2(\mu\text{-dppm})]$, has been prepared (by an entirely different route) and characterised fully.[16] This species was unique in being electron precise, but paramagnetic to the extent of two unpaired electrons. The ruthenium species **7**, by contrast, is diamagnetic, and clearly does not possess the near degeneracy of orbitals required to give the triplet molecule, but on the basis of spectroscopic data (IR and NMR) appears to be structurally similar to the osmium species, with equatorial phosphine and bridging tin groups.

It is noteworthy that reaction (5) was carried out under rather milder conditions than for (4), but nevertheless gave partial fragmentation of the ruthenium triangle. This may reflect an electronic effect of the dialkyltin ligands on the stability of the expected Ru_3 species. There is some supporting evidence for this view in the structure of **8**, in which the dialkyl-bridged Ru atoms are further apart than any of the other Ru–Ru bonds having the same bridging group in any of the hexanuclear cluster molecules.

In the light of these results it was interesting to examine the reactions of ruthenium dodecacarbonyl with Karsch's tin(II) species $Sn[CH(PPh_2)_2]_2$,[17] which has been shown to have three-co-ordinate tin in the solid state.[18] The carbonyl reacts with $Sn[CH(PPh_2)_2]_2$ in toluene at ambient temperature to give $[Ru_3(CO)_{12}(dppm)]$ in 96% yield. The lead analogue behaves similarly but the product was obtained in low yield. The isolation of the diphosphine adduct under such mild conditions is surprising: the free phosphine gives the product only in poor yields (together with other products) at elevated temperature, and requires 50 °C even when activated by an electron-transfer reagent, such as sodium–benzophenone.[19] These facts show that the reaction of the $Sn[CH(PPh_2)_2]_2$ reagent with ruthenium carbonyl cannot proceed by formation of free diphosphine. It presumably occurs *via* an intermediate ruthenium–tin species which breaks down. Unstable products are observed during the course of the reaction, but we have no evidence as to their composition, and the required protons are presumably taken up during chromatography, in view of the rigorously aprotic conditions required for the tin(II) reagent. Nevertheless the tin species functions as a rapid, mild and almost quantitative transfer reagent for the diphosphine. There is some generality to this behaviour, since the bis(diaryltin)-bridged compound **1** reacts also with $Sn[CH(PPh_2)_2]_2$ to give the diphosphine complex **7**, though this reaction required gentle warming and gave only moderate yields.

Structures of the new clusters

Full single-crystal structure analyses have been conducted on compounds **2**, **4**, **5** and **8**. Fig. 1 gives a geometrical survey for these compounds with framework bond lengths, and Figs. 2–5 illustrate the individual molecules. Table 3 compares bond lengths and other derived parameters for these clusters with those of the parent structure $(SnR'_2)_3$. Selected bond lengths and angles and atomic coordinates for **2**, **4**, **5** and **8** are provided in Tables 4–11. Table 3 shows that all the Ru–Ru bonds are lengthened with respect to the parent carbonyl [2.854(4) Å][20] as is found (with the single exception of μ-CO) when ligands bridge the Ru_3 triangle.

The structure of compound **2** confirms the planar hexametallic array, and the nearly (but not exactly) orthogonal disposition of the tin ligands with respect to this plane. This structural feature of the aryltin ligand generates a characteristic 'twist', which is remarkably consistent in all the structures we have studied. The asymmetric unit consists of one and a half trimer units. At room temperature the asymmetric unit for $(SnR'_2)_3$ corresponds to three trimer units, but on cooling to −50 °C the crystals adopt a structure having an asymmetric unit one third of this size.[15] We interpret this as a consequence of there being many conformers of the molecule corresponding to various arrangements of the $C_6H_2Pr^i_3$ groups having very similar energies, a single one of which is frozen out at low temperature. A similar effect is presumably responsible for the large size of the asymmetric unit in the crystals of **2**. Fig. 1 shows the metal geometries in these molecules compared with the others in this study. Both the triangles are isosceles, with a longer Ru–Ru distance of 2.960(3) (average) and a shorter Ru–Ru distance of 2.941(3) Å (average). The Ru–Sn distances do not show a consistent pattern, and all lie within the range 2.715(2)–2.734(2) Å. The pattern of 'twists' at the tin centres (defined as the dihedral angle between the planes containing the tin and its two attached carbon atoms, and the least-squares metal plane) shows a characteristic value of about 10° away from the normal.

The structures of the mixed-ligand clusters **4** and **5** enable a detailed comparison of the steric and electronic effects of the R and R′ ligands in otherwise identical molecules. Compound **4** is the second most sterically crowded of the clusters, and its most striking feature is the adoption of space group $P6_1$ or $P6_5$ in individual crystals, a result which can be directly traced to the presence of this 'twist' on the aryltin atoms. The chirality is apparently generated by the further asymmetry caused by having only two twisted ligands. This space group has not previously been observed for a metal cluster. The product, as expected, is obtained as a racemic mixture of the enantiomeric crystal forms. Owing to the long *c* axis, these crystals were particularly suitable for making a comparison of crystal data-collection methodologies. The results are in Table 12, which refers to four independent, fully refined structures. Data collections were performed on different crystals. In each case refinements were carried out in both space groups, $P6_1$ or $P6_5$, eight refinements in all. For each crystal the space group was assigned based on the refinement which gave the lower *R* value.

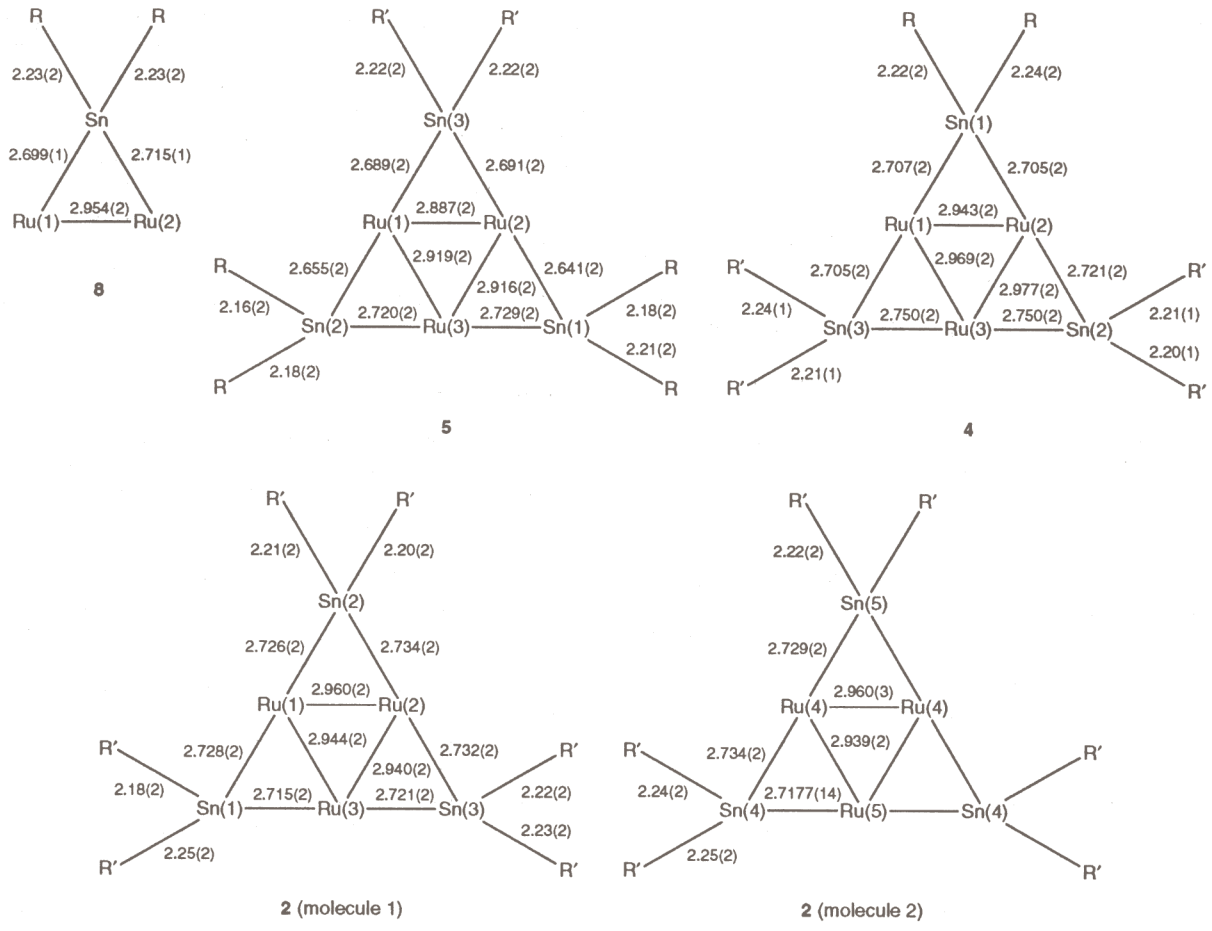

Fig. 1 Structures of compounds **2**, **4**, **5** and **8**, showing metal-framework bond lengths (Å). Selected framework bond angles (°) are: **2** (molecule 1), R′–Sn(1)–R′ 96.7(7), R′–Sn(2)–R′ 100.1(7), R′–Sn(3)–R′ 98.4(7); (molecule 2), R′–Sn(4)–R′ 99.2(7), R–Sn(5)–R′ 100.7(7); **4**, R–Sn(1)–R 96.8(6), R′–Sn(3)–R′ 97.3(4), R′–Sn(2)–R′ 98.8(5); **5**, R′–Sn(3)–R′ 100.8(7), R–Sn(2)–R 103.8(10), R–Sn(1)–R 105.2(8); **8**, R–Sn–R 111.4(8)

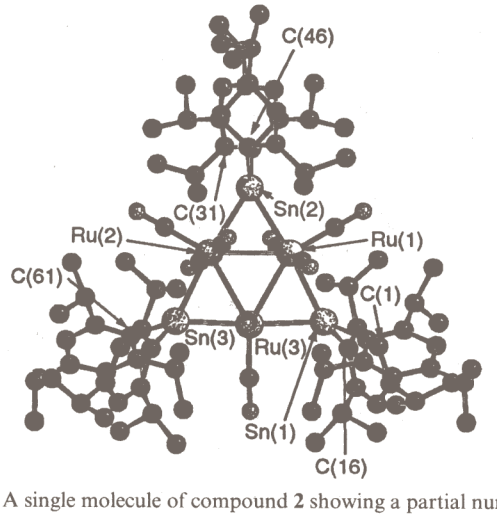

Fig. 2 A single molecule of compound **2** showing a partial numbering scheme

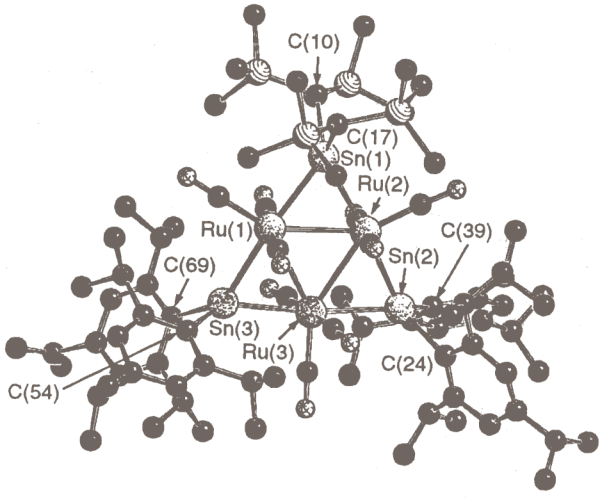

Fig. 3 A single molecule of compound **4** showing a partial numbering scheme

The best data set was obtained at −50 °C, using an image-plate system, and the derived parameters are remarkably consistent, with no clear source of systematic error. This is data set 2, which is referred to in the remainder of this paper. In **4** the Ru–Ru distances are comparable with those in the tris(diaryltin) compound **2**, but longer than those in the bis(dialkyltin)-mono(diaryltin) **5**, which is presumed to be a steric effect. The whole metal framework is isosceles with two mutually *trans* long Sn–Ru distances from the SnR'_2 ligands (Fig. 1). In contrast, compound **5** adopts a normal crystal packing, and this can probably be traced to the presence of only a single twisted aryltin group combined with the lower rigidity of the SnR_2 group. The Ru–Ru distances are shorter than in both **2** and **4**, but the feature of the overall isosceles metal framework is, curiously, retained, the two mutually *trans*-elongated Ru–Sn now being those with alkyl substituents on the tin atoms. It is therefore apparent that the overall molecular symmetry plays a role in determining this last feature, which is therefore neither steric nor associated with crystal packing.

As we have found for all cases in which tin metals bridge the sides of transition-metal clusters, the $CH(SiMe_3)_2$ (R) ligands on tin subtend an angle at the metal (the C–Sn–C angle) larger than that in the free (monomeric, gas phase) ligand (SnR_2) (97°)[21] as expected from a consideration of valence-shell electron-pair repulsions around the tin atom, but smaller

than in the crystalline dimer $[(SnR_2)_2]$ (112°)[22] in which the tin is three-co-ordinate, and in agreement with the steric compression around the four-co-ordinate tins. The behaviour of the SnR'_2 and SnR_2 ligands is distinctly different, as can be seen from the data in Table 3. While both the C–Sn–C angles and the twist angles show variation between different SnR_2 moieties, the corresponding parameters in the various SnR'_2 entities remains remarkably constant. Indeed, this invariance extends beyond the twist and C–Sn–C angles to the Sn–Sn distance in the trimer $(SnR'_2)_3$, which is constrained to be close to the Ru–Ru distances of the mixed-metal clusters.[10] It thus appears that the bulk of the SnR'_2 group effectively locks the geometry in all these molecules, *i.e.* the metal–metal spacing is determined by the 'bite' of the SnR'_2 ligand.

In the diruthenium cluster **8** the Ru–Ru bond is bridged by both a tin moiety and by the diphosphine. The substituents on both the P atoms and on the tin are essentially co-ordinated perpendicular to the plane of the Ru_2Sn triangle. The Ru–Ru bond is substantially longer than in the parent carbonyl, and at 2.954(2) Å is in the range expected for the SnR'_2 ligand; but in this case the distance is presumably determined by a complex mixture of factors including the effect of the tin bridge and the 'bite' of the bridging diphosphine ligand. The lack of steric strain seems to be indicated by the P–Ru–Ru angles of 91.4(1) and 91.0(1)°. The geometries of both the R_2Sn and dppm moieties are as expected from related structures, and the disposition of carbonyl groups about the ruthenium atoms is normal with two essentially collinear with the Ru–Ru vector and four essentially perpendicular to the metal plane.

In summary: (*i*) the Ru–Ru distances are all lengthened by varying amounts compared with those in the parent carbonyl; (*ii*) the overall metal shape consists of isosceles triangles in the mixed-ligand clusters; (*iii*) the twist angles between the C–Sn–C and the metal planes are about 10° from normal with SnR'_2, and significantly less for SnR_2; (*iv*) the Ru–Ru separations are remarkably close to the Sn–Sn lengths in the parent trimer $(SnR'_2)_3$; (*v*) the C–Sn–C ligand angles are much more sensitive to the environment in the case of the alkyl ligand than in the aryl; and (*vi*) these angles are smaller throughout for the SnR'_2 ligands, presumably because of steric compression caused by the bulkier aryl groups.

Experimental

Synthesis

The experimental techniques employed have been described

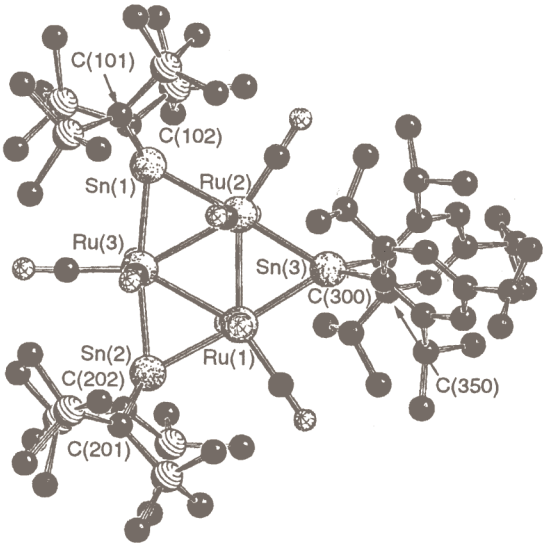

Fig. 4 A single molecule of compound **5** showing a partial numbering scheme

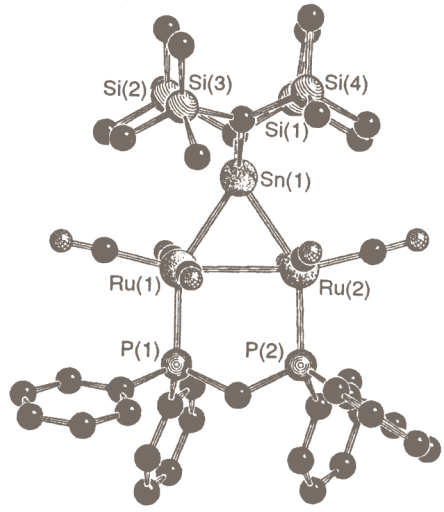

Fig. 5 A single molecule of compound **8** showing a partial numbering scheme

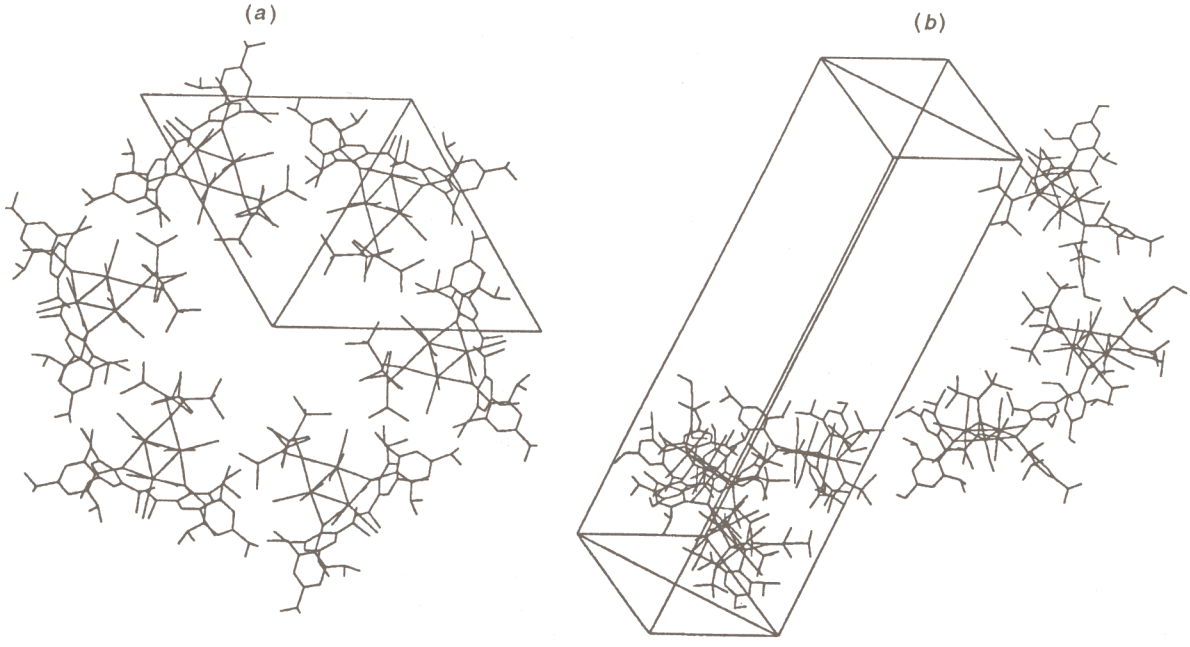

Fig. 6 The unit cell of compound **4** viewed down the *c* axis (*a*) and a perspective view (*b*)

Table 3 Comparison of bond lengths and derived parameters

	Compound				
	2	**4**	**5**	**8**	$(SnR'_2)_3$
Ru–Ru/Å	2.944(2)	2.943(2)	2.887(2)	2.954(2)	
	2.960(2)	2.969(2)	2.919(2)		
	2.940(2)	2.977(2)	2.916(2)		
	2.939(2)				
	2.960(3)				
Ru–Sn/Å	2.726(2)	2.707(2) $\}$ SnR_2	2.641(2) $\}$	2.699(1)	
	2.728(2)	2.705(2) $\}$	2.729(2) $\}$ SnR_2	2.715(1)	
	2.732(2)	2.721(2) $\}$	2.655(2) $\}$		
	2.734(2)	2.750(2) $\}$ SnR'_2	2.720(2) $\}$		
	2.715(2)	2.705(2) $\}$	2.691(2) $\}$ SnR'_2		
	2.721(2)	2.750(2) $\}$	2.689(2) $\}$		
	2.718(1)				
	2.729(2)				
	2.734(2)				
C–Sn–C/°	96.7(7)	96.8(6) SnR_2	103.8(10) $\}$ SnR_2	111.4(8)	105.3(5)
	100.1(7)	97.3(4) $\}$	105.2(8) $\}$		102.2(5)
	98.4(7)	98.8(5) $\}$ SnR'_2	100.8(7) SnR'_2		104.9(5)[a]
	99.2(7)				
	100.7(7)				
Twist angles[b]/°	82.93	88.8 SnR_2	88.76 $\}$ SnR_2		81.68
	(molecule 1)	80.1 $\}$	86.35 $\}$		80.8
	78.95	78.5 $\}$ SnR'_2	81.78 SnR'_2		78.49
	81.35				80.62
	79.80				81.08
	(molecule 2)				80.11
	79.54				81.94
					78.61[c]
Sn–C/Å	2.18(2)	2.22(2) $\}$ SnR_2	2.18(2) $\}$	2.23(2)	2.21(1)
	2.25(2)	2.24(2) $\}$	2.21(2) $\}$ SnR_2	2.23(2)	2.19(1)
	2.20(2)	2.21(1) $\}$	2.16(2) $\}$		2.15(1)
	2.21(2)	2.20(1) $\}$ SnR'_2	2.18(2) $\}$		2.19(1)
	2.22(2)	2.24(1) $\}$	2.22(2) $\}$ SnR'_2		2.19(1)
	2.23(2)	2.21(1) $\}$	2.22(2) $\}$		2.18(1)
	2.25(2)				
	2.24(2)				
	2.22(2)				

[a] Data from ref. 14. [b] The dihedral angle between each C–Sn–C plane and the least-squares plane through the six metal atoms. [c] From ref. 9.

Table 4 Selected bond lengths (Å) and angles (°) for compound **2**

Ru(1)–Sn(2)	2.726(2)	Ru(4)–Sn(5)	2.729(2)
Ru(1)–Sn(1)	2.728(2)	Ru(4)–Sn(4)	2.734(2)
Ru(1)–Ru(3)	2.944(2)	Ru(4)–Ru(4^I)	2.960(3)
Ru(1)–Ru(2)	2.960(2)	Sn(1)–C(11)	2.18(2)
Ru(2)–Sn(3)	2.732(2)	Sn(1)–C(21)	2.25(2)
Ru(2)–Sn(2)	2.734(2)	Sn(2)–C(31)	2.20(2)
Ru(2)–Ru(3)	2.940(2)	Sn(2)–C(41)	2.21(2)
Ru(3)–Sn(1)	2.715(2)	Sn(3)–C(51)	2.22(2)
Ru(3)–Sn(3)	2.721(2)	Sn(3)–C(61)	2.23(2)
Ru(5)–Sn(4)	2.7177(14)	Sn(4)–C(81)	2.25(2)
Ru(5)–Sn(4)	2.7178(14)	Sn(4)–C(71)	2.24(2)
Ru(5)–Ru(4)	2.939(2)	Sn(5)–C(91)	2.22(2)
Sn(2)–Ru(1)–Ru(2)	57.29(5)	Ru(4^I)–Ru(5)–Ru(4)	60.48(7)
Ru(3)–Ru(1)–Ru(2)	59.72(5)	Sn(4)–Ru(4)–Ru(5)	57.12(4)
Sn(3)–Ru(2)–Ru(3)	57.20(5)	Sn(5)–Ru(4)–Ru(4^I)	57.15(4)
Sn(2)–Ru(2)–Ru(1)	57.05(5)	Ru(5)–Ru(4)–Ru(4^I)	59.76(4)
Ru(3)–Ru(2)–Ru(1)	59.86(5)	C(11)–Sn(1)–C(21)	96.7(7)
Sn(3)–Ru(3)–Ru(2)	57.56(5)	C(31)–Sn(2)–C(41)	100.1(7)
Sn(1)–Ru(3)–Ru(1)	57.47(5)	C(51)–Sn(3)–C(61)	98.4(7)
Ru(2)–Ru(3)–Ru(1)	60.41(5)	C(81)–Sn(4)–C(71)	99.2(7)
Sn(4^I)–Ru(5)–Ru(4^I)	57.64(5)	C(91)–Sn(5)–C(91^I)	100.7(8)
Sn(4)–Ru(5)–Ru(4)	57.64(5)		

Symmetry transformations used to generate equivalent atoms: I $-x+1, y, -z+\frac{1}{2}$.

Table 5 Selected bond lengths (Å) and angles (°) for compound **4**

Sn(1)–Ru(1)	2.707(2)	Sn(1)–Ru(2)	2.705(2)
Sn(1)–C(10)	2.22(2)	Sn(1)–C(17)	2.24(2)
Sn(2)–Ru(2)	2.721(2)	Sn(2)–Ru(3)	2.750(2)
Sn(2)–C(24)	2.21(1)	Sn(2)–C(39)	2.20(1)
Sn(3)–Ru(1)	2.705(2)	Sn(3)–Ru(3)	2.750(2)
Sn(3)–C(54)	2.24(1)	Sn(3)–C(69)	2.21(1)
Ru(1)–Ru(2)	2.943(2)	Ru(1)–Ru(3)	2.969(2)
Ru(2)–Ru(3)	2.977(2)		
Ru(2)–Sn(1)–Ru(1)	65.9(1)	Ru(3)–Ru(1)–Ru(2)	60.5(1)
C(17)–Sn(1)–C(10)	96.8(6)	Ru(1)–Ru(2)–Sn(1)	57.1(1)
Ru(3)–Sn(2)–Ru(2)	65.9(1)	Ru(3)–Ru(2)–Sn(2)	57.5(1)
C(39)–Sn(2)–C(24)	98.8(5)	Ru(3)–Ru(2)–Ru(1)	60.2(1)
Ru(3)–Sn(3)–Ru(1)	65.9(1)	Ru(1)–Ru(3)–Sn(3)	56.3(1)
C(69)–Sn(3)–C(54)	97.3(4)	Ru(2)–Ru(3)–Sn(2)	56.6(1)
Ru(2)–Ru(1)–Sn(1)	57.0(1)	Ru(2)–Ru(3)–Ru(1)	59.3(1)
Ru(3)–Ru(1)–Sn(3)	57.7(1)		

elsewhere.[23] The NMR spectra were measured on Bruker MSL 300, WP80, JEOL GX270 or EX400 machines.

$[Ru_3(CO)_{10}(\mu\text{-}SnR'_2)_2]$ 1 and $[Ru_3(CO)_9(\mu\text{-}SnR'_2)_3]$ 2. (*a*) *Using the dissociated tin reagent*. The freshly prepared tin dimer $(SnR'_2)_2$[5] (*ca.* 4.5 mmol) in thf (45 cm^3) at −50 °C was added dropwise to a stirred suspension of ruthenium dodecacarbonyl (0.5 g, 0.77 mmol) in toluene (50 cm^3) at room temperature. The solution was stirred overnight, remaining unreacted carbonyl was filtered off, and the filtrate evaporated to dryness under vacuum. The residue was taken up in hexane (20 cm^3), and separated by flash chromatography on silica, changing the eluent from hexane–dichloromethane (90:10) to (80:20). Two fractions were collected, and crystallised from hexane affording compounds **1** (0.44 g, 35%) and **2** (0.74 g, 45%).

(*b*) *Using the* cyclo-*tristannane*. Ruthenium dodecacarbonyl (0.2 g, 0.31 mmol) and the tristannane $(SnR'_2)_3$ (0.2 g, 0.12

Table 6 Selected bond lengths (Å) and angles (°) for compound **5**

Sn(1)–C(102)	2.18(2)	Ru(2)–Sn(3)	2.691(2)
Sn(1)–C(101)	2.21(2)	Ru(2)–Ru(3)	2.916(2)
Sn(1)–Ru(2)	2.641(2)	Sn(2)–C(202)	2.16(2)
Sn(1)–Ru(3)	2.729(2)	Sn(2)–C(201)	2.18(2)
Ru(1)–Sn(2)	2.655(2)	Sn(2)–Ru(3)	2.720(2)
Ru(1)–Sn(3)	2.689(2)	Sn(3)–C(350)	2.22(2)
Ru(1)–Ru(2)	2.887(2)	Sn(3)–C(300)	2.22(2)
Ru(1)–Ru(3)	2.919(2)		
C(102)–Sn(1)–C(101)	105.2(8)	C(202)–Sn(2)–C(201)	103.8(10)
Ru(2)–Sn(1)–Ru(3)	65.76(4)	Ru(1)–Sn(2)–Ru(3)	65.78(4)
Sn(3)–Ru(1)–Ru(2)	57.58(4)	C(350)–Sn(3)–C(300)	100.8(7)
Sn(2)–Ru(1)–Ru(3)	58.19(4)	Ru(1)–Sn(3)–Ru(2)	64.91(4)
Ru(2)–Ru(1)–Ru(3)	60.29(4)	Sn(1)–Ru(3)–Ru(2)	55.67(4)
Sn(3)–Ru(2)–Ru(1)	57.51(4)	Sn(2)–Ru(3)–Ru(1)	56.03(4)
Sn(1)–Ru(2)–Ru(3)	58.57(4)	Ru(2)–Ru(3)–Ru(1)	59.30(4)
Ru(1)–Ru(2)–Ru(3)	60.41(4)		

Table 7 Selected bond lengths (Å) and angles (°) for compound **8**

Ru(1)–Ru(2)	2.954(2)	Ru(2)–Sn	2.715(1)
Ru(1)–P(1)	2.358(4)	Sn–C(50)	2.23(2)
Ru(1)–Sn	2.699(1)	Sn–C(51)	2.23(2)
Ru(2)–P(2)	2.374(4)		
Sn–Ru(1)–Ru(2)	57.2(1)	P(1)–Ru(1)–Ru(2)	91.4(1)
Sn–Ru(2)–Ru(1)	56.7(1)	P(2)–Ru(2)–Ru(1)	91.0(1)
Ru(2)–Sn–Ru(1)	66.1(1)	C(50)–Sn–C(51)	111.4(8)

mmol) were dissolved in thf (55 cm^3) and the solution warmed slowly to reflux (45 min) then allowed to cool. Thin-layer chromatography (hexane–dichloromethane, 95:5) revealed the tristannane (R_f 0.57), compounds **1** (R_f 0.36) and **2** (R_f 0.42) and an unknown material (R_f 0.31). The solution was reduced in volume to *ca.* 10 cm^3 and stored at −20 °C overnight. After filtering off the precipitated tristannane, the solution was evaporated to dryness, dissolved in the minimum volume of hexane, and chromatographed on silica using hexane, affording after recrystallisation from hexane, **1** (0.167 g, 33%) and **2** (0.30 g, 46%). The third, purple product was eluted with hexane–dichloromethane (90:10) but there was insufficient material for characterisation.

$[Ru_3(CO)_9(\mu\text{-}SnR_2)_3]$ 6. Ruthenium dodecacarbonyl (0.3 g, 0.46 mmol) in toluene (150 cm^3) was added dropwise to a diethyl ether solution of the tin reagent (1.5 g, 0.337 mmol) at room temperature. Solvent was removed under vacuum (leaving toluene as the main solvent), and the mixture heated (60–70 °C) until the carbonyl had been consumed (monitored by TLC), then cooled. After removal of toluene under vacuum, the residue was dissolved in hexane and chromatographed on silica, affording the bis(tin) cluster **3** (0.37 g, 56%), and compound **6** (0.17 g, 28%) after recrystallisation from hexane.

$[Ru_3(CO)_9(\mu\text{-}SnR_2)_2(\mu\text{-}SnR'_2)]$ 5. To $[Ru_3(CO)_{10}(SnR_2)_2]$ (0.3 g, 0.2 mmol) in toluene (50 cm^3) was added $(SnR'_2)_3$ (0.5 g, 0.316 mmol). The mixture was heated to just below reflux (2 h). Toluene was removed under vacuum, the residue dissolved in the minimum volume of hexane (*ca.* 7 cm^3) and chromatographed on silica using hexane. The red fraction was collected, reduced to small volume (*ca.* 5 cm^3) and cooled to −20 °C. Red crystals of compound **5** (0.35 g, 90%) were filtered off.

$[Ru_3(CO)_9(\mu\text{-}SnR_2)(\mu\text{-}SnR'_2)_2]$ 4. The compound SnR_2 (0.08 g, 0.18 mmol) in toluene (30 cm^3) was added dropwise to a stirred solution of $[Ru_3(CO)_{10}(\mu\text{-}SnR'_2)_2]$ (0.1 g, 0.061 mmol) in toluene (30 cm^3). After warming the solution (50 °C, 45 min), then cooling, the volume was reduced to *ca.* 5 cm^3 under vacuum and subjected to flash chromatography on a silica column using hexane as eluent. The single red band eluted was recrystallised from hexane to give compound **4** (0.112 g, 90%).

$[Ru_3(CO)_8(\mu\text{-}SnR'_2)_2(dppm)]$ 7. The compound $[Ru_3(CO)_{10}(dppm)]$ (0.25 g, 0.26 mmol) and $(SnR'_2)_3$ (1 g, 0.63 mmol) were heated (20 min, 90 °C) in toluene (100 cm^3) with stirring. Toluene was removed under vacuum, the residue taken up in the minimum volume of hexane (*ca.* 20 cm^3), and subjected to flash chromatography on silica. Successive elution with (*i*) hexane, (*ii*) hexane–dichloromethane (90:10) and (*iii*) hexane–dichloromethane (70:30) afforded respectively $(SnR'_2)_3$, $[Ru_3(CO)_{10}(SnR'_2)_2]$ with $[Ru_3(CO)_9(SnR'_2)_3]$, and finally $[Ru_3(CO)_8(\mu\text{-}SnR'_2)_2(dppm)]$ **7** as the major product. The latter was recrystallised from hexane (*ca.* 10 cm^3) at −20 °C, yield 0.31 g (60%).

$[Ru_2(CO)_6(\mu\text{-}SnR_2)(dppm)]$ 8. The compound SnR_2 (0.5 g, 1.14 mmol) in ether (25 cm^3) was added to $[Ru_3(CO)_{10}(dppm)]$ (0.2 g, 0.2 mmol) in toluene (100 cm^3). The mixture was reduced in volume to 75 cm^3 (predominantly toluene) and heated (70 °C, 30 min), then allowed to cool. The solution was further reduced to *ca.* 30 cm^3, tin starting material was filtered off, and the filtrate pumped to dryness. The residue was taken up in the minimum volume of toluene (*ca.* 10 cm^3) and subjected to flash chromatography on silica (hexane eluent). The hexametallic Ru_3Sn_3 cluster was eluted, the eluate changed to hexane–dichloromethane (75:25) and the orange-brown fraction collected. After reduction in volume under vacuum and storage at −20 °C pale yellow compound **8** crystallised (0.16 g, 66%).

Crystallography

All data were collected using graphite-monochromated Mo-Kα radiation (λ 0.710 73 Å).

Compound 2. *Crystal data.* $C_{99}H_{138}O_9Ru_3Sn_3$, M = 2131.39, monoclinic, space group $P2/c$, a = 31.60(4), b = 17.21(2), c = 34.47(4) Å, β = 104.31(14)°, U = 18 163.3 $Å^3$ (by least-squares refinement on diffractometer angles for 25 centred reflections), Z = 6, D_c = 1.169 g cm^{-3}, $F(000)$ = 6516. Red, air-stable blocks, crystal dimensions 0.1 × 0.2 × 0.2 mm. μ(Mo-Kα) = 10.16 mm^{-1}.

Data collection and processing. Stoe Stadi-4 diffractometer, ω–2θ mode. 19 038 Unique reflections measured, 8472 having $|F| > 5\sigma(F)$. The data were corrected for decay and absorption using an empirical correction (both small). The structure was solved by the Patterson method of SHELXS 86 [24] and refined by full-matrix least squares with 731 parameters. Only the Ru and Sn atoms were refined anisotropically. Hydrogen atoms were placed geometrically and given a common thermal parameter of 0.07 $Å^2$. The program SHELX 76 [25] was used until the final refinement, which was carried out with SHELXL 93 [26] (refined on F^2). The final R factor was 0.0925 for data having $I > 2\sigma(I)$.

Compound 4. *Crystal data.* $C_{83}H_{130}O_9Ru_3Si_4Sn_3$, M = 2043.566, hexagonal, space group $P6_5$ (no. 170), a = 19.735(2), c = 49.431(8) Å, U = 16 672.3 $Å^3$ (by least-squares refinement using 558 reflections, at 223 K), Z = 6, D_c = 1.221 g cm^{-3}, $F(000)$ = 1038, μ(Mo-Kα) = 1.73 cm^{-1}. Orange needle-shaped crystals, dimensions 0.1 × 0.1 × 0.3 mm.

Data collection and processing. Stoe IPDS, 0.5° rotation with 0.002° φ increment, 600 s exposure, 42 692 reflections measured (maximum 2θ of 48°), 8360 unique (R_{merge} = 0.0661), giving 7576 with $|F_o| > 4\sigma|F_o|$. Patterson method of SHELXS 86 followed by Fourier-difference synthesis. Blocked full-matrix least-squares refinement using the SHELX 76 [25] program and refining on F (R = 0.484) (936 parameters). All non-hydrogen atoms anisotropic and hydrogens in calculated

Table 8 Fractional atomic coordinates ($\times 10^4$) for compound **2**

Atom	x	y	z	Atom	x	y	z
Ru(1)	7 889(1)	3 005(1)	164(1)	C(45)	8 660(9)	6 365(14)	454(7)
Ru(2)	8 170(1)	2 993(1)	−594(1)	C(46)	8 390(7)	5 754(11)	332(6)
Ru(3)	8 034(1)	1 522(1)	−208(1)	C(47)	9 161(8)	4 603(13)	−157(7)
Ru(5)	5 000	4 427(1)	2 500	C(48)	9 363(12)	7 161(19)	539(11)
Ru(4)	4 668(1)	5 902(1)	2 736(1)	C(49)	7 950(8)	5 755(12)	420(7)
Sn(1)	7 791(1)	1 595(1)	493(1)	C(410)	9 263(8)	4 823(14)	−516(7)
Sn(2)	8 034(1)	4 332(1)	9 785(1)	C(411)	9 554(8)	4 245(14)	138(8)
Sn(3)	8 285(1)	1 574(1)	−908(1)	C(412)	9 784(16)	7 030(26)	699(14)
Sn(4)	4 378(1)	4 486(1)	2 920(1)	C(413)	9 339(13)	7 686(21)	248(11)
Sn(5)	5 000	7 235(1)	2 500	C(414)	8 026(10)	5 602(16)	856(8)
O(1)	6 920(5)	2 709(8)	−215(5)	C(415)	7 699(10)	6 493(15)	301(9)
O(2)	7 628(6)	3 883(10)	835(6)	C(51)	8 934(6)	1 276(10)	−1 009(5)
O(3)	8 854(5)	3 322(8)	557(4)	C(52)	9 235(7)	810(12)	−740(7)
O(4)	7 201(5)	3 317(8)	−989(4)	C(53)	9 604(7)	538(11)	−868(7)
O(5)	8 434(5)	3 832(9)	−1 273(5)	C(54)	9 672(7)	688(11)	−1 237(6)
O(6)	9 141(5)	2 687(8)	−217(4)	C(55)	9 374(7)	1 185(12)	−1 474(7)
O(7)	7 144(5)	1 520(8)	−816(5)	C(56)	9 005(6)	1 490(10)	−1 370(6)
O(8)	8 031(5)	−234(8)	−201(5)	C(57)	9 222(8)	628(12)	−321(7)
O(9)	8 919(5)	1 511(8)	418(5)	C(58)	10 049(7)	347(12)	−1 400(7)
O(10)	4 022(5)	6 228(8)	1 924(5)	C(59)	8 732(7)	2 048(10)	−1 671(6)
O(11)	5 287(5)	5 613(8)	3 558(5)	C(510)	9 611(8)	951(12)	−14(7)
O(12)	4 077(6)	6 757(10)	3 154(6)	C(511)	9 155(9)	−210(14)	−262(8)
O(13)	4 165(5)	4 445(8)	1 812(5)	C(512)	10 455(12)	416(21)	−1 089(11)
O(14)	5 000	2 666(13)	2 500	C(513)	10 025(11)	−485(16)	−1 420(9)
C(1)	7 275(7)	2 845(10)	−81(6)	C(514)	8 964(9)	2 760(13)	−1 683(8)
C(2)	7 742(8)	3 539(13)	578(7)	C(515)	8 560(8)	1 704(14)	−2 071(7)
C(3)	8 495(7)	3 159(11)	396(6)	C(61)	7 867(6)	1 012(10)	−1 452(6)
C(4)	7 549(7)	3 160(10)	−844(6)	C(62)	7 570(7)	1 395(11)	−1 751(6)
C(5)	8 332(7)	3 526(11)	−1 007(6)	C(63)	7 391(7)	1 033(11)	−2 113(6)
C(6)	8 773(6)	2 810(10)	−332(5)	C(64)	7 499(6)	304(10)	−2 205(6)
C(7)	7 478(8)	1 559(12)	−578(7)	C(65)	7 777(6)	−96(10)	−1 889(6)
C(8)	8 022(6)	466(10)	−213(5)	C(66)	7 972(6)	216(10)	−1 509(5)
C(9)	8 586(7)	1 551(10)	163(6)	C(67)	7 420(7)	2 215(11)	−1 693(7)
C(10)	4 262(7)	6 075(10)	2 214(6)	C(68)	7 335(8)	−116(12)	−2 594(7)
C(20)	5 081(7)	5 731(10)	3 244(6)	C(69)	8 255(7)	−302(11)	−1 188(6)
C(30)	4 317(8)	6 473(12)	2 986(7)	C(610)	7 572(8)	2 782(12)	−1 951(7)
C(40)	4 480(7)	4 426(10)	2 063(6)	C(611)	6 917(7)	2 223(13)	−1 764(7)
C(50)	5 000	3 349(17)	2 500	C(612)	6 886(8)	−426(14)	−2 617(8)
C(11)	7 167(7)	1 250(11)	606(6)	C(613)	7 348(9)	364(15)	−2 930(8)
C(12)	6 842(7)	792(12)	346(6)	C(614)	7 973(8)	−911(12)	−1 082(7)
C(13)	6 492(10)	489(15)	467(9)	C(615)	8 625(8)	−666(13)	−1 330(8)
C(14)	6 430(8)	688(13)	843(8)	C(71)	3 738(7)	3 922(11)	2 640(6)
C(15)	6 729(9)	1 130(14)	1 095(9)	C(72)	3 360(7)	4 308(11)	2 450(6)
C(16)	7 097(7)	1 450(12)	965(7)	C(73)	2 955(7)	3 963(11)	2 366(6)
C(17)	6 839(7)	635(12)	−94(6)	C(74)	2 909(9)	3 223(14)	2 478(8)
C(18)	5 999(13)	379(21)	959(13)	C(75)	3 293(7)	2 796(12)	2 668(6)
C(19)	7 386(8)	2 001(12)	1 267(7)	C(76)	3 693(6)	3 109(10)	2 751(5)
C(110)	6 917(9)	−235(14)	−183(8)	C(77)	3 390(8)	5 138(12)	2 287(7)
C(111)	6 455(8)	955(13)	−370(7)	C(78)	2 471(8)	2 797(13)	2 404(7)
C(112)	5 605(15)	651(24)	791(14)	C(79)	4 083(7)	2 594(12)	2 920(6)
C(113)	6 093(15)	−421(23)	1 056(13)	C(710)	3 190(8)	5 174(13)	1 833(7)
C(114)	7 557(8)	1 607(13)	1 655(7)	C(711)	3 181(8)	5 708(13)	2 497(7)
C(115)	7 132(8)	2 739(12)	1 320(7)	C(712)	2 117(10)	3 289(16)	2 470(9)
C(21)	8 218(6)	1 063(10)	1 049(6)	C(713)	2 351(10)	2 463(15)	2 003(8)
C(22)	8 517(7)	1 491(11)	1 335(6)	C(714)	4 048(9)	2 227(13)	3 306(7)
C(23)	8 703(8)	1 128(13)	1 700(7)	C(715)	4 133(8)	2 004(13)	2 629(7)
C(24)	8 616(8)	373(12)	1 773(7)	C(81)	4 427(7)	4 182(11)	3 563(6)
C(25)	8 369(7)	−49(13)	1 476(7)	C(82)	4 083(8)	4 367(12)	3 715(7)
C(26)	8 171(7)	280(12)	1 111(7)	C(83)	4 057(11)	4 076(17)	4 081(10)
C(27)	8 626(8)	2 338(12)	1 301(7)	C(84)	4 390(10)	3 609(15)	4 281(8)
C(28)	8 816(8)	35(14)	2 179(7)	C(85)	4 717(10)	3 407(15)	4 155(8)
C(29)	7 903(7)	−254(12)	784(7)	C(86)	4 762(8)	3 711(13)	3 774(7)
C(210)	8 485(10)	2 904(15)	1 565(8)	C(87)	3 729(7)	4 931(12)	3 516(7)
C(211)	9 117(8)	2 406(14)	1 339(8)	C(88)	4 372(12)	3 240(21)	4 736(10)
C(212)	8 705(10)	415(15)	2 529(8)	C(89)	5 211(9)	3 510(14)	3 698(8)
C(213)	9 300(11)	−44(20)	2 271(11)	C(810)	3 797(11)	5 586(17)	3 770(10)
C(214)	7 552(9)	−640(15)	950(8)	C(811)	3 279(8)	4 591(14)	3 464(8)
C(215)	8 196(8)	−857(13)	673(7)	C(812)	4 538(18)	3 792(28)	4 997(16)
C(31)	7 554(6)	5 166(10)	−551(6)	C(813)	3 986(13)	2 839(22)	4 703(12)
C(32)	7 137(7)	5 231(10)	−490(6)	C(814)	5 269(10)	2 636(15)	3 605(9)
C(33)	6 883(8)	5 897(12)	−644(6)	C(815)	5 553(10)	3 888(16)	3 986(9)
C(34)	7 043(7)	6 474(11)	−864(6)	C(91)	5 462(6)	8 059(9)	2 885(5)
C(35)	7 452(7)	6 385(12)	−914(6)	C(92)	5 650(7)	8 651(11)	2 659(6)
C(36)	7 702(8)	5 731(13)	−778(7)	C(93)	5 858(7)	9 284(12)	2 872(6)
C(37)	6 898(7)	4 652(11)	−295(6)	C(94)	5 910(7)	9 326(12)	3 271(7)
C(38)	6 759(9)	7 187(13)	−1 036(8)	C(95)	5 756(7)	8 787(12)	3 487(7)

Table 8 (*continued*)

Atom	*x*	*y*	*z*	Atom	*x*	*y*	*z*
C(39)	8 147(7)	5 703(12)	−880(6)	C(96)	5 548(7)	8 117(11)	3 276(6)
C(310)	6 499(7)	4 365(12)	−556(7)	C(97)	5 597(7)	8 626(12)	2 211(6)
C(311)	6 803(9)	4 968(15)	103(8)	C(98)	6 137(9)	10 043(15)	3 497(9)
C(312)	6 962(11)	7 882(17)	−806(10)	C(99)	5 425(7)	7 519(11)	3 555(6)
C(313)	6 647(10)	7 283(17)	−1 458(9)	C(910)	5 399(8)	9 331(12)	2 009(7)
C(314)	8 402(9)	6 408(13)	−752(8)	C(911)	6 050(8)	8 481(13)	2 140(7)
C(315)	8 097(9)	5 522(14)	−1 308(7)	C(912)	5 872(13)	10 705(20)	3 427(12)
C(41)	8 533(7)	5 143(11)	122(6)	C(913)	6 583(11)	10 120(18)	3 470(10)
C(42)	8 946(7)	5 191(12)	60(6)	C(914)	5 098(8)	7 789(13)	3 768(7)
C(43)	9 233(9)	5 837(13)	196(7)	C(915)	5 815(8)	7 198(13)	3 847(7)
C(44)	9 065(10)	6 451(15)	384(8)				

Table 9 Fractional atomic coordinates for compound **4**

Atom	*x*	*y*	*z*	Atom	*x*	*y*	*z*
Sn(1)	0.828 35(5)	0.425 41(5)	0.106 74(4)	C(32)	1.164 9(10)	0.492 7(11)	0.161 0(3)
Sn(2)	1.040 83(4)	0.336 05(5)	0.084 31(4)	C(33)	1.400 7(9)	0.457 0(12)	0.123 2(4)
Sn(3)	0.764 66(4)	0.134 74(5)	0.134 75(4)	C(34)	1.417 2(12)	0.414 3(17)	0.142 6(5)
Ru(1)	0.789 87(6)	0.278 08(6)	0.120 95(4)	C(35)	1.446 9(14)	0.481 5(25)	0.100 7(6)
Ru(2)	0.940 52(6)	0.388 78(6)	0.095 95(4)	C(36)	1.151 9(8)	0.251 3(8)	0.081 2(3)
Ru(3)	0.906 01(5)	0.227 92(5)	0.109 85(4)	C(37)	1.194 4(9)	0.254 7(11)	0.054 3(3)
C(1)	0.831 3(7)	0.302 8(7)	0.156 4(2)	C(38)	1.144 7(9)	0.185 2(9)	0.098 1(3)
O(1)	0.855 6(6)	0.314 6(5)	0.179 1(2)	C(39)	1.076 2(7)	0.339 5(7)	0.042 1(2)
C(2)	0.690 6(8)	0.252 1(7)	0.133 1(3)	C(40)	1.043 3(7)	0.273 9(7)	0.024 7(2)
O(2)	0.627 6(6)	0.235 2(7)	0.140 3(2)	C(41)	1.080 3(8)	0.276 2(8)	0.000 2(2)
C(3)	0.754 9(7)	0.255 0(7)	0.085 2(3)	C(42)	1.145 9(8)	0.342 4(9)	−0.008 2(2)
O(3)	0.733 5(6)	0.241 6(5)	0.062 8(2)	C(43)	1.177 4(7)	0.408 1(8)	0.008 1(3)
C(4)	1.010 4(9)	0.488 8(8)	0.083 6(3)	C(44)	1.141 1(7)	0.406 6(8)	0.033 1(2)
O(4)	1.058 8(6)	0.552 9(6)	0.077 2(2)	C(45)	0.966 5(8)	0.199 6(7)	0.030 9(2)
C(5)	0.972 2(7)	0.420 6(8)	0.132 4(3)	C(46)	0.979 2(12)	0.129 4(9)	0.037 2(4)
O(5)	0.991 6(6)	0.446 6(6)	0.154 1(2)	C(47)	0.902 8(9)	0.179 3(9)	0.009 1(3)
C(6)	0.902 9(7)	0.349 1(7)	0.059 4(3)	C(48)	1.190 6(10)	0.344 4(10)	−0.033 8(3)
O(6)	0.885 0(6)	0.327 9(6)	0.038 0(2)	C(49)	1.213 8(20)	0.412 5(18)	−0.050 2(5)
C(7)	0.967 4(8)	0.277 0(7)	0.141 8(3)	C(50)	1.262 2(14)	0.342 3(18)	−0.028 3(5)
O(7)	1.011 3(6)	0.306 0(6)	0.159 3(2)	C(51)	1.178 6(8)	0.486 4(8)	0.047 9(3)
C(8)	0.843 1(8)	0.174 3(8)	0.078 9(3)	C(52)	1.266 8(8)	0.522 2(10)	0.054 6(3)
O(8)	0.800 1(5)	0.138 7(5)	0.061 6(2)	C(53)	1.164 3(9)	0.543 6(9)	0.032 5(3)
C(9)	0.937 7(8)	0.153 7(8)	0.111 2(3)	C(54)	0.740 3(7)	0.098 0(6)	0.178 2(2)
O(9)	0.958 4(7)	0.108 9(7)	0.112 1(3)	C(55)	0.799 7(7)	0.103 9(8)	0.196 7(2)
C(10)	0.763 7(9)	0.451 9(7)	0.075 9(3)	C(56)	0.777 8(9)	0.066 0(9)	0.220 4(3)
Si(1)	0.654 1(3)	0.397 5(3)	0.081 7(1)	C(57)	0.696 2(10)	0.023 3(9)	0.229 0(3)
C(11)	0.599 8(9)	0.287 7(9)	0.074 6(3)	C(58)	0.642 7(8)	0.025 3(8)	0.211 9(2)
C(12)	0.634 0(12)	0.410 7(11)	0.117 6(4)	C(59)	0.661 9(7)	0.060 7(7)	0.186 9(2)
C(13)	0.603 3(14)	0.437 7(13)	0.059 6(5)	C(60)	0.885 7(7)	0.148 9(8)	0.190 2(2)
Si(2)	0.794 2(3)	0.470 5(3)	0.039 2(1)	C(61)	0.930 0(9)	0.210 5(9)	0.211 2(3)
C(14)	0.902 4(12)	0.511 8(10)	0.032 1(3)	C(62)	0.919 6(10)	0.095 1(12)	0.186 6(4)
C(15)	0.779 5(14)	0.550 4(11)	0.026 2(4)	C(63)	0.666 9(12)	−0.023 5(10)	0.256 0(3)
C(16)	0.736 4(13)	0.383 0(10)	0.017 7(3)	C(64)	0.685 7(21)	−0.086 3(14)	0.257 8(5)
C(17)	0.842 8(9)	0.517 1(8)	0.136 5(3)	C(65)	0.685 5(16)	0.028 5(14)	0.279 7(4)
Si(3)	0.935 8(3)	0.615 2(3)	0.129 7(1)	C(66)	0.595 9(7)	0.059 8(8)	0.170 4(2)
C(18)	1.030 9(10)	0.618 8(9)	0.139 1(4)	C(67)	0.533 8(8)	−0.022 2(9)	0.165 3(3)
C(19)	0.939 6(14)	0.639 2(10)	0.093 4(4)	C(68)	0.564 6(11)	0.106 3(12)	0.185 0(3)
C(20)	0.931 2(12)	0.697 2(10)	0.147 6(4)	C(69)	0.679 4(7)	0.021 1(7)	0.116 7(2)
Si(4)	0.814 3(3)	0.498 0(3)	0.172 8(1)	C(70)	0.689 0(7)	−0.044 4(7)	0.124 5(3)
C(21)	0.734 5(10)	0.395 6(9)	0.181 3(3)	C(71)	0.631 3(8)	−0.120 7(8)	0.118 6(3)
C(22)	0.900 1(11)	0.521 1(14)	0.196 3(4)	C(72)	0.563 8(9)	−0.132 5(9)	0.104 1(4)
C(23)	0.767 6(12)	0.556 4(13)	0.182 6(4)	C(73)	0.556 6(9)	−0.070 3(8)	0.095 0(3)
C(24)	1.153 7(7)	0.369 6(7)	0.104 0(2)	C(74)	0.613 2(7)	0.006 2(7)	0.101 2(2)
C(39)	1.076 2(7)	0.339 5(7)	0.042 1(2)	C(75)	0.761 2(8)	−0.034 0(8)	0.139 3(3)
C(54)	0.740 3(7)	0.098 0(6)	0.178 2(2)	C(76)	0.740 2(10)	−0.077 9(8)	0.165 5(3)
C(69)	0.679 4(7)	0.021 1(7)	0.116 7(2)	C(77)	0.806 3(9)	−0.059 5(9)	0.120 8(4)
C(25)	1.199 2(8)	0.440 8(8)	0.119 1(2)	C(78)	0.498 1(10)	−0.218 3(10)	0.098 5(5)
C(26)	1.276 2(8)	0.466 0(8)	0.125 8(3)	C(79)	0.441 2(17)	−0.252 8(18)	0.115 5(5)
C(27)	1.312 6(8)	0.426 5(10)	0.117 8(3)	C(80)	0.507 8(12)	−0.249 8(11)	0.072 9(4)
C(28)	1.271 4(8)	0.356 0(11)	0.103 6(3)	C(81)	0.601 4(8)	0.069 2(8)	0.089 9(2)
C(29)	1.191 1(7)	0.326 7(8)	0.096 5(2)	C(82)	0.526 6(9)	0.065 0(9)	0.100 6(3)
C(30)	1.164 5(7)	0.488 6(9)	0.129 6(3)	C(83)	0.601 8(11)	0.064 9(11)	0.058 2(3)
C(31)	1.207 0(10)	0.572 4(9)	0.119 6(3)				

positions with those in similar environments given common refined thermal parameters. The final Fourier-difference map had a highest peak of 0.66 e Å^{-3}.

Compound 5. *Crystal data.* $C_{67}H_{122}O_9Ru_3Si_8Sn_3$, M = 1955.65, triclinic, space group $P\bar{1}$ (no. 2), a = 14.986(5), b = 15.143(5), c = 23.035(5) Å, α = 107.99(6), β = 89.75(6), γ =

Table 10 Fractional atomic coordinates ($\times 10^4$) for compound **5**

Atom	*x*	*y*	*z*	Atom	*x*	*y*	*z*
Sn(1)	1271(1)	2040(1)	2510(1)	C(302)	4400(21)	−1253(22)	892(11)
Ru(1)	1251(1)	−1101(1)	2541(1)	C(306)	2649(17)	−2114(18)	1146(10)
Ru(2)	2352(1)	1118(1)	2571(1)	C(102)	1077(17)	2308(21)	1652(10)
Sn(2)	−814(1)	−2132(1)	2461(1)	C(307)	2113(18)	−2335(21)	549(10)
Sn(3)	3330(1)	37(1)	2576(1)	C(353)	5994(19)	709(21)	4203(11)
Ru(3)	86(1)	−45(1)	2494(1)	C(13)	1362(11)	−2292(13)	2535(8)
Si(11)	2090(6)	2758(6)	1172(3)	C(112)	2480(28)	4146(31)	1160(19)
Si(12)	2865(6)	4626(6)	3531(3)	C(211)	−2171(24)	−4457(22)	3753(13)
Si(21)	−1241(5)	−3618(6)	3382(3)	C(231)	−331(19)	−4351(19)	1239(11)
Si(22)	−2161(6)	−2119(7)	3724(3)	C(233)	−2633(21)	−5837(20)	996(12)
Si(23)	−1573(6)	−4418(6)	1058(3)	C(141)	785(32)	4262(25)	2023(17)
Si(13)	594(7)	3434(7)	3796(3)	C(123)	3516(19)	4872(21)	2883(13)
Si(14)	120(7)	2669(10)	1577(4)	C(113)	1559(27)	1756(29)	377(12)
O(21)	2385(9)	1952(10)	3955(6)	C(363)	3659(23)	−2467(20)	2977(11)
O(31)	226(10)	564(12)	3873(6)	C(305)	5168(16)	605(19)	1880(10)
O(11)	596(10)	−1944(10)	1142(6)	C(23)	3617(16)	2345(17)	2681(8)
O(12)	1700(11)	−270(10)	3950(6)	C(142)	−1021(27)	1954(48)	1893(22)
Si(24)	−3124(6)	−3713(8)	1424(4)	C(313)	6608(17)	1925(21)	2810(11)
O(22)	2122(11)	266(11)	1179(6)	C(212)	−1167(19)	−4600(19)	2698(11)
O(32)	−319(11)	−712(12)	1095(6)	C(359)	6856(32)	893(30)	4621(19)
C(21)	2372(12)	1608(15)	3451(9)	C(213)	−42(25)	−2800(21)	3885(11)
C(11)	867(12)	−1610(14)	1653(9)	C(201)	−1597(18)	−2733(21)	3175(11)
C(31)	229(13)	379(14)	3375(8)	C(312)	5667(17)	1689(22)	2338(12)
C(111)	3361(15)	2924(18)	1395(10)	C(232)	−1587(24)	−4320(23)	258(10)
C(357)	5565(15)	3224(16)	4049(10)	C(143)	−374(28)	2381(35)	776(14)
O(13)	1419(11)	−2992(12)	2529(9)	C(131)	353(27)	4506(26)	3933(14)
C(22)	2183(13)	596(15)	1699(10)	C(132)	−698(22)	2134(26)	3613(16)
C(12)	1536(14)	−557(16)	3430(10)	C(303)	5409(19)	−470(25)	985(12)
C(352)	5695(15)	1460(17)	4282(9)	C(364)	4980(21)	−1579(23)	2352(13)
C(354)	5496(19)	−211(22)	3707(14)	C(314)	5992(23)	2612(22)	2136(13)
O(23)	4417(10)	3137(11)	2751(7)	C(222)	−3405(24)	−3099(30)	3832(17)
C(32)	−118(13)	−462(14)	1606(9)	C(202)	−1846(18)	−3385(22)	1602(10)
C(358)	2611(17)	−3110(18)	1176(10)	C(133)	1221(33)	3638(31)	4581(12)
C(362)	4234(18)	−1467(20)	2758(12)	C(223)	−2309(24)	−1093(29)	3577(17)
C(356)	4672(14)	2153(14)	4035(8)	C(361)	7679(28)	1861(50)	4825(22)
C(101)	1508(16)	3500(16)	3264(8)	C(241)	−3970(33)	−4584(41)	718(19)
C(308)	4281(16)	2269(18)	4627(9)	C(33)	−1207(15)	−131(16)	2414(10)
C(355)	4712(16)	−432(18)	3265(10)	O(33)	−1943(14)	−141(17)	2374(10)
C(121)	3613(24)	4430(19)	4031(10)	C(309)	6189(29)	−675(35)	544(14)
C(304)	5743(17)	448(19)	1430(12)	C(221)	−1304(29)	−1435(29)	4511(12)
C(122)	2984(25)	5920(21)	3999(12)	C(360)	6489(32)	514(48)	5124(26)
C(351)	4901(13)	1276(14)	3864(8)	C(310)	5963(43)	−490(49)	27(26)
C(300)	4153(14)	−217(17)	1794(8)	C(242)	−3272(39)	−2622(50)	1713(31)
C(350)	4416(13)	333(15)	3361(8)	C(243)	−3875(25)	−4744(41)	1880(19)
C(301)	3739(14)	−1173(17)	1295(9)	C(311)	5787(25)	−1743(41)	276(19)

Table 11 Fractional atomic coordinates for compound **8**

Atom	*x*	*y*	*z*	Atom	*x*	*y*	*z*
Ru(1)	0.087 30(11)	0.381 42(8)	0.216 21(7)	C(10)	−0.141 0(9)	0.501 3(9)	0.129 2(8)
Ru(2)	0.313 16(10)	0.474 30(8)	0.328 46(7)	C(11)	−0.192 1(9)	0.505 3(9)	0.065 3(8)
C(100)	−0.018 4(17)	0.317 9(13)	0.270 3(9)	C(12)	−0.123 3(9)	0.575 9(9)	0.036 5(8)
C(101)	−0.031 0(16)	0.296 0(13)	0.132 9(12)	C(13)	−0.003 4(9)	0.642 4(9)	0.071 5(8)
C(102)	0.199 4(15)	0.436 0(14)	0.165 4(13)	C(14)	0.226 7(9)	0.700 4(8)	0.427 9(5)
C(103)	0.453 6(15)	0.497 8(13)	0.396 1(11)	C(15)	0.241 2(9)	0.660 0(8)	0.482 5(5)
C(104)	0.195 6(16)	0.419 9(12)	0.383 4(10)	C(16)	0.192 3(9)	0.695 4(8)	0.539 6(5)
C(105)	0.425 1(15)	0.499 2(12)	0.266 1(12)	C(17)	0.128 9(9)	0.771 3(8)	0.542 2(5)
O(100)	−0.085 2(11)	0.277 6(9)	0.297 0(8)	C(18)	0.114 4(9)	0.811 7(8)	0.487 7(5)
O(101)	−0.102 3(13)	0.249 3(11)	0.085 4(8)	C(19)	0.163 4(9)	0.776 2(8)	0.430 6(5)
O(102)	0.256 4(13)	0.470 1(12)	0.134 7(7)	C(20)	0.422 6(7)	0.761 5(6)	0.364 2(6)
O(103)	0.539 9(11)	0.510 2(10)	0.435 4(7)	C(21)	0.473 1(7)	0.771 5(6)	0.307 7(6)
O(104)	0.135 7(14)	0.390 2(10)	0.416 0(8)	C(22)	0.577 0(7)	0.858 4(6)	0.315 7(6)
O(105)	0.495 2(14)	0.516 2(10)	0.235 3(7)	C(23)	0.630 4(7)	0.935 2(6)	0.380 1(6)
P(1)	0.042 5(4)	0.545 8(3)	0.241 5(2)	C(24)	0.579 9(7)	0.925 2(6)	0.436 6(6)
P(2)	0.285 9(4)	0.646 7(3)	0.351 1(2)	C(25)	0.476 0(7)	0.838 3(6)	0.428 6(6)
Sn	0.237 16(8)	0.267 11(7)	0.245 86(5)	C(52)	0.366 1(21)	0.245 3(17)	0.420 3(13)
C(50)	0.148 1(15)	0.147 8(11)	0.294 1(9)	C(53)	0.321 7(28)	0.025 2(23)	0.336 1(17)
C(51)	0.354 9(16)	0.204 2(19)	0.177 3(13)	C(54)	0.146 9(31)	0.072 3(24)	0.420 2(19)
Si(1)	0.240 8(5)	0.120 0(4)	0.362 2(3)	C(55)	0.087 2(31)	−0.074 6(24)	0.185 4(19)
Si(2)	0.020 8(6)	0.024 0(4)	0.230 9(4)	C(56)	−0.080 1(19)	0.049 8(15)	0.165 0(12)
Si(3)	0.298 6(7)	0.157 1(7)	0.084 8(4)	C(57)	−0.076 7(49)	−0.029 1(41)	0.285 2(29)
Si(4)	0.517 9(5)	0.218 9(4)	0.210 8(4)	C(58)	0.384 1(57)	0.288 5(44)	0.064 1(33)
C(1)	0.185 4(13)	0.663 0(11)	0.281 8(9)	C(59)	0.157 1(27)	0.159 0(23)	0.049 7(17)
C(2)	−0.062 2(10)	0.580 0(9)	0.295 7(6)	C(60)	0.375 6(25)	0.074 6(20)	0.032 8(15)
C(3)	−0.074 3(10)	0.538 9(9)	0.350 0(6)	C(61)	0.578 2(27)	0.305 8(22)	0.300 6(16)
C(4)	−0.147 2(10)	0.571 8(9)	0.395 6(6)	C(62)	0.551 5(32)	0.094 5(26)	0.196 0(20)

Table 11 (*continued*)

Atom	*x*	*y*	*z*	Atom	*x*	*y*	*z*
C(5)	−0.208 1(10)	0.645 8(9)	0.386 9(6)	C(63)	0.627 9(36)	0.307 2(29)	0.161 8(22)
C(6)	−0.196 0(10)	0.686 9(9)	0.332 6(6)	C(300)	0.457 2(86)	0.731 1(67)	0.114 9(49)
C(7)	−0.123 1(10)	0.654 0(9)	0.287 0(6)	C(301)	0.602 6(58)	0.675 1(45)	0.121 9(34)
C(8)	0.047 7(9)	0.638 3(9)	0.135 4(8)	C(302)	0.492 0(71)	0.702 3(55)	0.103 5(41)
C(9)	−0.021 1(9)	0.567 8(9)	0.164 2(8)	C(303)	0.358 3(69)	0.769 2(52)	0.098 2(40)

Table 12 Comparison of data collections for compound **4**

	Collection			
	1	2	3	4
Metal framework geometry (distances in Å, angles in °)				
Ru(1)–Ru(2)	2.942(4)	2.943(2)	2.941(3)	2.928(7)
Ru(2)–Ru(3)	2.975(2)	2.977(2)	2.970(3)	2.961(7)
Ru(3)–Ru(1)	2.969(3)	2.969(2)	2.971(3)	2.960(7)
Sn(1)–Ru	2.705(2), 2.704(3)	2.707(2), 2.705(2)	2.702(3), 2.771(3)	2.698(7), 2.685(7)
Sn(2)–Ru	2.719(3), 2.746(4)	2.721(2), 2.750(2)	2.713(3), 2.760(3)	2.713(7), 2.726(6)
Sn(3)–Ru	2.705(2), 2.748(4)	2.705(2), 2.750(2)	2.722(3), 2.753(3)	2.696(7), 2.750(6)
Sn(1)–C	2.23(3), 2.22(2)	2.22(2), 2.24(2)	2.23(2), 2.21(2)	2.19(5), 2.23(7)
Sn(2)–C	2.23(3), 2.20(2)	2.21(1), 2.20(1)	2.20(1), 2.28(2)	2.20(3), 2.20(4)
Sn(3)–C	2.23(2), 2.18(3)	2.24(1), 2.21(1)	2.24(2), 2.23(2)	2.22(4), 2.27(4)
Ru–Sn(1)–Ru	65.9(1)	65.9(1)	65.8(1)	65.9(2)
Ru–Sn(2)–Ru	66.0(1)	65.9(1)	65.7(1)	66.0(2)
Ru–Sn(3)–Ru	66.0(1)	65.9(1)	65.7(1)	65.8(2)
C–Sn(1)–C	98.1(9)	96.8(6)	96.8(9)	96(2)
C–Sn(2)–C	96(1)	98.8(5)	98.8(6)	98(1)
C–Sn(3)–C	96.7(9)	97.3(4)	99.4(6)	99(1)
Twist angles *				
Sn(1)/metals	89.1	88.8	89.0	87.4
Sn(2)/metals	78.5	78.5	79.4	78.6
Sn(3)/metals	79.6	80.1	78.4	78.9
Data collection parameters				
Detector system	Stoe image plate	Stoe image plate	Mar image plate	CAD4
T/°C	−50	−50	Room	20
Total reflections	20 000	42 692	3508	5974
Maximum 2θ/°	48	48	35	40
Unique reflections	8239	8360	3508	5331
R_{merge}	0.1324	0.0661	0	0.0745
Observed reflections	6130	7576	2979	2618
Structure refinement				
Space group	$P6_1$	$P6_5$	$P6_5$	$P6_1$
R	0.0719	0.0484	0.0480	0.0816
R'	0.0753	0.0494	0.0441	0.0828
Goodness of fit	1.4100	1.8532	2.1533	1.0995
No. parameters	960	936	415	415
No. data	5736	7356	3233	2691
Atoms anisotropic	All non-hydrogen	All non-hydrogen	Ru, Sn, Si	Ru, Sn, Si
Solvent	Five half-occupied positions refined	None located	None refined	None refined

* Between metal planes defined as the dihedral angle between the C–Sn–C plane and the Ru_3Sn_3 metal plane.

119.99(6)°, $U = 4234.2$ Å^3, $Z = 2$, $D_c = 1.534$ g cm^{-3}, $F(000) = 1980$. Stable red prisms. Crystal size 0.1 × 0.1 × 0.15 mm.

Data collection and processing. Mar Research image-plate scanner (small plate version), 95 2° frames with an exposure time of 10 min per frame. Data were processed with the Mar Research versions of XDS and XSCALE[27] to give 11 579 unique observations (R_{merge} 0.0405). Another crystal had previously been measured on a CAD-4 diffractometer, giving 10 737 independent reflections (R_{merge} 0.0185) of which 7374 had $|F| > 4\sigma(F)$. However the quality of this data set was inadequate to locate all the carbon atom positions satisfactorily. The triclinic cell can be transformed metrically to give a monoclinic lattice but the structure cannot be satisfactorily refined in the higher symmetry.

Structure solution and refinement. The structure was solved using the Patterson method of SHELXS 86 and refined using the program SHELXL 93 and MAR image-plate data to a final *R* value of 0.0810, goodness of fit on F^2 1.116. Anisotropic thermal parameters were used for all non-hydrogen atoms, incorporating isotropic restraints. The largest peak in the final difference map had a height of 1.648 e Å^{-3}.

Compound 8. *Crystal data.* $C_{45}H_{60}O_6P_2Ru_2Si_4Sn$, *M* 1192.087, triclinic, space group $P\bar{1}$ (no. 2), $Z = 2$, $D_c = 1.36$ g cm^{-3}, $a = 11.338(2)$, $b = 13.626(4)$, $c = 20.739(2)$ Å, $\alpha = 105.86(2)$, $\beta = 97.67(1)$, $\gamma = 104.77(2)$°, $U = 2908(1)$ Å^3 (by least-squares refinement of the setting angles of 25 reflections, $16 < \theta < 18$°), $F(000) = 1204$, μ(Mo-Kα) = 10.09 cm^{-1}.

Data collection and processing. 4893 Reflections were measured ($1 < \theta < 20$°) using a yellow oblong crystal, approximate dimensions 0.15 × 0.15 × 0.25 mm, on an Enraf-Nonius CAD-4 diffractometer (ω–2θ scans). The data were corrected for decay and absorption (empirical correction using

three reflections with φ *ca.* 90°, minimum transmission 60%), and then merged to give 4692 unique reflections (R_{merge} = 0.0336), of which 4258 had $|F_o| > 4\sigma|F_o|$.

Structure solution and refinement. The structure was solved by the Patterson routine of SHELXS 86 and refined by full-matrix least-squares analysis on F using the SHELX 76[25] program to $R = 0.0865$ (328 parameters). The heavy atoms were refined with anisotropic thermal parameters, the hydrogens were placed geometrically, those in similar environments being given common thermal parameters [CH_2, 0.02(1); phenyl CH, 0.15(1); ligand CH, 0.2(1); CH_3, 0.31(3) Å^2]. An area of solvent was also located, but could not be assigned; the four positions of highest electron density in this area were refined as half-occupied carbons. The weighting scheme was refined to give a flat analysis of variance ($R' = 0.0989$). The highest peak in the final difference map was 1.55 e Å^{-3}; all peaks over 1 e Å^{-3} were found to be in the vicinity of the Ru and Sn atoms.

Complete atomic coordinates, thermal parameters and bond lengths and angles have been deposited at the Cambridge Crystallographic Data Centre. See instructions for Authors, *J. Chem. Soc., Dalton Trans.*, 1996, Issue 1.

Acknowledgements

We thank the Krieble fund for financial assistance (to M. A. C., M. M. D. and M. B. P.), EOLAS and the Federation of Irish Chemical Industries for support (to M. A. C.), and the EC for financial support. Drs. P. R. Raithby (University of Cambridge) and P. R. Evans (Laboratory for Molecular Biology, Cambridge) are thanked for helpful discussions and the generous provision of instrument time. Emilio Tedesco (University of Bologna) and Yan Zubavichus (Higher Chemical Institute, Moscow) contributed to the crystallography as part of the EC Erasmus programme 'Crystallography' (E. T.), and sponsored by Sun Microsystems and Rotary International (Y. Z.). Dr. E. Keller (Schakal), Professor W. Kabsch (XDS and XSCALE) and Professor G. Sheldrick (SHELX 76, SHELXL 93 and SHELXS 86) are thanked for permission to use their crystallographic software.

References

1 Part 4, N. C. Burton, C. J. Cardin, D. J. Cardin, B. Twamley and Y. Zubavichus, *Organometallics*, 1995, **14**, 5708.
2 K. H. Whitmire, *J. Coord. Chem.*, 1988, **17**, 95.
3 J. A. Cabeza, R. J. Francis and V. Riera, *Inorg. Chem.*, 1994, **33**, 5952; S. W. Lee, K. Yang, J. A. Martin, S. G. Bott and M. G. Richmond, *Inorg. Chim. Acta*, 1995, **232**, 57 and refs. therein.
4 See, for example, R. A. T. Gould, K. L. Craighead, J. S. Wiley and L. H. Pignolet, *Inorg. Chem.*, 1995, **34**, 2902; M. Shieh, T.-F. Tang, S.-M. Peng and G.-H. Lee, *Inorg. Chem.*, 1995, **35**, 2797.
5 (*a*) C. J. Cardin, D. J. Cardin, N. B. Kelly, G. A. Lawless and M. B. Power, *J. Organomet. Chem.*, 1988, **341**, 447; (*b*) C. J. Cardin, D. J. Cardin, G. A. Lawless and M. B. Power, *Proc. R. Ir. Acad., Sect. B*, 1989, **89**, 399.
6 C. J. Cardin, D. J. Cardin, G. A. Lawless, J. M. Power, M. B. Power and M. B. Hursthouse, *J. Organomet. Chem.*, 1987, **325**, 203.
7 C. J. Cardin, D. J. Cardin, M. A. Convery and M. M. Devereux, *J. Chem. Soc., Chem. Commun.*, 1991, 687 and refs. therein.
8 C. J. Cardin, D. J. Cardin and M. B. Power, *J. Organomet. Chem.*, 1993, **462**, C27.
9 S. Masamune and L. R. Sita, *J. Am. Chem. Soc.*, 1985, **107**, 6390.
10 F. J. Brady, C. J. Cardin, D. J. Cardin, M. A. Convery, M. M. Devereux and G. A. Lawless, *J. Organomet. Chem.*, 1991, **241**, 199.
11 A. Brookes, S. A. R. Knox and F. G. A. Stone, *J. Chem. Soc. A*, 1971, 3469.
12 S. A. R. Knox and F. G. A. Stone, *J. Chem. Soc. A*, 1971, 2874.
13 J. Howard, S. A. R. Knox, F. G. A. Stone and P. Woodward, *Chem. Commun.*, 1970, 1477.
14 J. Howard and P. Woodward, *J. Chem. Soc. A*, 1971, 3648.
15 C. J. Cardin, M. A. Convery and D. Fenske, unpublished work.
16 R. A. Bartlett, C. J. Cardin, D. J. Cardin, G. A. Lawless, J. M. Power and P. P. Power, *J. Chem. Soc., Chem. Commun.*, 1988, 312.
17 H. H. Karsch, A. Appelt and G. Muller, *Organometallics*, 1986, **5**, 1664.
18 A. L. Balch and D. E. Oram, *Organometallics*, 1986, **5**, 2159.
19 M. I. Bruce, *Coord. Chem. Rev.*, 1987, **76**, 1.
20 M. R. Churchill, F. J. Hollander and J. P. Hutchinson, *Inorg. Chem.*, 1977, **16**, 2655.
21 T. Fjeldberg, A. Haaland, M. F. Lappert, B. E. R. Schilling, R. Seip and A. J. Thorne, *J. Chem. Soc., Chem. Commun.*, 1982, 1407.
22 D. E. Goldberg, D. H. Harris, M. F. Lappert and K. M. Thomas, *J. Chem. Soc., Chem. Commun.*, 1976, 256.
23 C. J. Cardin, D. J. Cardin, H. E. Parge and A. C. Sullivan, *J. Chem. Soc., Dalton Trans.*, 1986, 2315.
24 G. M. Sheldrick, SHELXS 86, University of Göttingen, 1986.
25 G. M. Sheldrick, SHELX 76, University of Cambridge, 1976.
26 G. Sheldrick, SHELXL 93, University of Göttingen, 1993.
27 W. Kabsch, *J. Appl. Crystallogr.*, 1993, **26**, 795.

Received 31*st July* 1995; *Paper* 5/05078B